

Budget-Sensitive Discovery Scoring: A Formally Verified Framework for Evaluating AI-Guided Scientific Selection

Abhinaba Basu*

Pavan Chakraborty†

Abstract

Scientific discovery increasingly relies on AI systems to select candidates for expensive experimental validation, yet no principled, budget-aware evaluation framework exists for comparing selection strategies—a gap intensified by large language models (LLMs), which generate plausible scientific proposals without reliable downstream evaluation. We introduce the Budget-Sensitive Discovery Score (BSDS), a formally verified metric—20 theorems machine-checked by the Lean 4 proof assistant—that jointly penalizes false discoveries (λ -weighted FDR) and excessive abstention (γ -weighted coverage gap) at each budget level. Its budget-averaged form, the Discovery Quality Score (DQS), provides a single summary statistic that no proposer can inflate by performing well at a cherry-picked budget.

As a case study, we apply BSDS/DQS to a question of broad interest: *do LLMs add marginal value to an existing ML pipeline for drug discovery candidate selection?* We evaluate 39 proposers—11 mechanistic variants, 14 zero-shot LLM configurations, and 14 few-shot LLM configurations—using SMILES (Simplified Molecular Input Line Entry System) representations on MoleculeNet HIV (41,127 compounds, 3.5% active, 1,000 bootstrap replicates) under both random and scaffold splits. Three findings emerge. *First*, the simple RF-based Greedy-ML proposer achieves the best DQS (-0.046), outperforming all MLP variants and LLM configurations; additional MLP reranking layers degrade rather than improve the RF’s discriminative ranking. *Second*, no LLM surpasses the Greedy-ML baseline under either zero-shot or few-shot evaluation on HIV or Tox21—establishing that LLMs provide no marginal value over an existing trained classifier, the realistic deployment scenario. *Third*, the proposer hierarchy generalizes across five MoleculeNet benchmarks spanning 0.18%–46.2% prevalence, a non-drug AV safety domain, and a 9×7 grid of penalty parameters ($\tau \geq 0.636$, mean $\tau = 0.863$). The framework applies in principle to any setting where candidates are selected under budget constraints and asymmetric error costs, as demonstrated here across pharmaceutical screening and autonomous vehicle safety triage.

1 Introduction

Scientific discovery increasingly depends on AI systems—from virtual screening pipelines in drug discovery to anomaly detectors in autonomous vehicle safety—to select candidates for expensive experimental validation. Yet evaluation of these selection systems remains surprisingly ad hoc. Standard classification metrics (AUROC, F_1) integrate over all operating points, obscuring performance at the specific budget where decisions are actually made. Enrichment factors capture early retrieval but ignore false-discovery costs. No existing metric jointly models budget constraints, asymmetric error costs, and the option to abstain—three properties that are fundamental to real-world discovery campaigns.

*Indian Institute of Information Technology Allahabad (IIITA) and National Institute of Electronics & Information Technology (NIELIT). ORCID: 0000-0003-1575-4107.

†Indian Institute of Information Technology Allahabad (IIITA). ORCID: 0000-0002-9260-1131.

The evaluation paradigm gap. Consider drug discovery, where a single approved therapeutic costs an estimated \$2.6 billion (Vamathevan et al., 2019) with a 90% attrition rate between Phase I and market. A pharmaceutical company screening for HIV inhibitors selects perhaps 500 out of 40,000 candidates for wet-lab confirmation. Three evaluation gaps emerge. First, discovery operates under *budget constraints*: the relevant question is not “how accurately does the model predict activity?” but “among the candidates selected within budget, how many are true hits?” Second, errors are *asymmetrically costly*: a false positive wastes an experimental slot costing thousands of dollars, while a false negative is a difficult-to-quantify opportunity cost. Third, proposers should be rewarded for *calibrated abstention*: declining to commit on ambiguous candidates is preferable to guessing.

These gaps apply beyond drug discovery. Any domain where candidates are selected from a pool under resource constraints—materials screening, safety scenario prioritization, clinical trial site selection—faces the same evaluation challenge. Large language models (LLMs) have amplified the urgency: ChemCrow (Bran et al., 2024), Coscientist (Boiko et al., 2023), and FunSearch (Romera-Paredes et al., 2024) demonstrate that LLMs can generate plausible scientific proposals, but determining whether those proposals improve *downstream experimental outcomes* requires evaluation metrics that existing benchmarks cannot provide.

Prior work in context. Virtual screening metrics—enrichment factors (EF) (Jain and Nicholls, 2008), BEDROC (Truchon and Bayly, 2007), AUROC, and MCC (Chicco and Jurman, 2020)—provide mature evaluation criteria but are budget-agnostic and lack formal guarantees. MoleculeNet (Wu et al., 2018) standardized molecular benchmarking but evaluates models on fixed metrics without budget or abstention modeling. Retrieval-augmented generation (RAG) (Lewis et al., 2020) improves LLM factuality but does not address downstream decision quality. Active learning (Settles, 2009; Reker and Schneider, 2015; Graff et al., 2021) provides principled acquisition strategies but lacks a unified terminal evaluation metric. Jablonka et al. (2024) found that LLMs achieve competitive knowledge retrieval but struggle with quantitative molecular reasoning. Ma et al. (2024) surveyed over 50 LLM systems for drug design but noted a pervasive absence of standardized evaluation frameworks. Formal verification has been applied to neural network safety (Selsam et al., 2017) but not to discovery evaluation metrics. Our work bridges these streams: a formally verified evaluation framework applied to the most prominent use case—LLM-guided drug discovery.

This paper. We present the Budget-Sensitive Discovery Score (BSDS), a formally verified evaluation metric (20 theorems machine-checked by the Lean 4 proof assistant (de Moura and Ullrich, 2021)) that jointly penalizes false discoveries (λ -weighted FDR) and excessive abstention (γ -weighted coverage gap) at each budget level. Its budget-averaged form, the Discovery Quality Score (DQS), provides a single summary statistic robust to budget cherry-picking.

As a case study, we apply BSDS/DQS to a question of broad interest: *given an existing ML pipeline for drug discovery, do LLMs add marginal value to candidate selection under realistic budget constraints?* The comparison is deliberately asymmetric: a pharmaceutical team already has a trained surrogate model (here, a Random Forest on 33,000+ compounds), and the practical question is whether an LLM—given SMILES strings and, optionally, ML predictions—can improve the selection. We do not test whether LLMs can replace a trained classifier from scratch; we test whether they contribute additional value beyond one. This asymmetry is intentional and reflects real deployment: the ML model *has* been trained on available data, and the question is whether an LLM—with zero-shot or few-shot access—adds orthogonal signal. Strategies requiring RAG, chain-of-thought, or tool-augmented LLM access remain important open directions (Section 5.7).

Contributions.

1. **Formally verified evaluation framework.** BSDS/DQS provides budget-sensitive, asymmetric-cost evaluation with 20 machine-checked theorems (boundedness, monotonicity, oracle dominance, Bayes-optimal abstention). The framework is applicable to any budget-constrained selection problem with binary outcomes.
2. **Comprehensive proposer evaluation.** We evaluate 39 proposers—11 mechanistic variants (8 base strategies plus 3 ablation controls), 14 zero-shot LLM configurations, and 14 few-shot LLM configurations—on MoleculeNet HIV (41,127 compounds, 1,443 actives, 3.5% prevalence) using 1,000 bootstrap replicates across six budget levels, under both random and scaffold CV splits.
3. **RF baseline outperforms MLP rerankers.** The simple RF-based Greedy-ML proposer (DQS = -0.046) outperforms all MLP variants and LLM configurations. Additional MLP reranking layers degrade the RF’s discriminative ranking, and a deployment simulation confirms 96% hit rate at $B = 50$.
4. **LLMs do not add marginal value.** No LLM surpasses the Greedy-ML baseline under either zero-shot or few-shot evaluation on HIV or Tox21, despite access to the same RF predictions.
5. **Budget-sensitive evaluation reveals invisible tradeoffs.** BSDS/DQS distinguish between 7 proposers that share identical EF and AUROC values (all using the same RF surrogate), capturing the precision–recall–abstention tradeoff invisible to conventional enrichment analysis.
6. **Robust generalization across datasets and domains.** The proposer hierarchy generalizes across five MoleculeNet benchmarks spanning 0.18%–46.2% prevalence, a non-drug AV safety domain, and a 9×7 grid of (λ, γ) parameters ($\tau \geq 0.636$, mean $\tau = 0.863$).

Paper organization. Section 2 recapitulates the BSDS/DQS framework. Section 3 describes the 39 proposer strategies and experimental setup. Section 4 presents the main results. Section 5 discusses implications, limitations, and future work. Section 6 concludes.

2 BSDS Framework

This section provides a concise recap of the Budget-Sensitive Discovery Score (BSDS) and the Discovery Quality Score (DQS). For complete definitions, proofs, and the decision-theoretic derivation, we refer the reader to the companion metric paper (Basu and Chakraborty, 2025); all 20 theorems have been machine-checked in Lean 4 (de Moura and Ullrich, 2021) and are independently verifiable via `lake build`.

2.1 Definition

Let $\mathcal{X} = \{x_1, \dots, x_N\}$ be a finite candidate pool with binary labels $g(x_i) \in \{0, 1\}$ and prevalence $p = |\{x : g(x) = 1\}|/N$. A proposer policy π selects a subset $S \subseteq \mathcal{X}$ with $|S| \leq B$ (the experimental budget) and may designate an abstention set $A \subseteq \mathcal{X} \setminus S$. Let $\mathcal{H} = \{x : g(x) = 1\}$ denote the true hits. The three component rates measure recall, false-discovery rate, and the fraction of candidates that receive a definitive decision (selected or explicitly rejected, as opposed

to abstained):

$$\text{HR@}B = \frac{|S \cap \mathcal{H}|}{|\mathcal{H}|} \quad (\text{recall over hits}), \quad (1)$$

$$\text{FDR@}B = \frac{|S \setminus \mathcal{H}|}{\max(|S|, 1)} \quad (\text{false-positive fraction}), \quad (2)$$

$$\text{Cov@}B = \frac{|S| + |\mathcal{X} \setminus S \setminus A|}{N} \quad (\text{decisiveness}). \quad (3)$$

Definition 1 (Budget-Sensitive Discovery Score). *For false-discovery penalty $\lambda \geq 0$ and abstention penalty $\gamma \geq 0$:*

$$\boxed{\text{BSDS}(B) = \text{HR@}B - \lambda \cdot \text{FDR@}B - \gamma \cdot (1 - \text{Cov@}B)} \quad (4)$$

The parameter λ encodes the cost of a wasted experimental validation relative to the benefit of a true discovery: setting $\lambda = 2$ means a false positive costs twice the value of a confirmed hit. The parameter γ penalizes leaving candidates unevaluated, preventing proposers from achieving artificially high precision by committing only on obvious cases.

Definition 2 (Discovery Quality Score). *Given evaluation budgets $\mathcal{B} = \{B_1, \dots, B_M\}$:*

$$\text{DQS} = \frac{1}{|\mathcal{B}|} \sum_{B \in \mathcal{B}} \text{BSDS}(B). \quad (5)$$

DQS averages BSDS across the full budget spectrum, ensuring that a proposer cannot achieve a high score by performing well at a single cherry-picked budget. More generally, DQS can incorporate tail-risk, oracle-gap, and minimax-regret penalties (see Basu and Chakraborty (2025)); in this paper we use the budget-averaged form for clarity.

2.2 Key Properties

We state four core properties that govern the behavior of BSDS as an evaluation metric. Each has been mechanically verified in Lean 4; proofs are provided in Basu and Chakraborty (2025).

P1. Boundedness. $-(\lambda + \gamma) \leq \text{BSDS} \leq 1$ for all valid inputs. This ensures a well-calibrated utility scale for cross-proposer comparison.

P2. Incentive compatibility. BSDS is strictly increasing in HR, strictly decreasing in FDR (when $\lambda > 0$), and non-decreasing in Cov (when $\gamma > 0$). No paradoxical regime exists in which a proposer could improve precision yet decrease its BSDS.

P3. Random degeneracy. A random proposer achieves $\text{BSDS}_{\text{rand}} = B/N - \lambda(1 - p) - \gamma(1 - B/N)$. For the HIV dataset ($p \approx 0.035$, $\lambda = 1.0$), this gives $\text{DQS} \approx -0.819$, consistent with the observed value.

P4. Oracle dominance. The oracle proposer (selecting true positives first) achieves maximal BSDS among all non-empty selections at any fixed coverage. For any policy π , $\text{BSDS}_\pi \leq \text{BSDS}_{\text{oracle}}$.

Two additional properties are particularly relevant for LLM evaluation:

Bayes-optimal abstention. At full coverage, a non-empty selection dominates full abstention ($\text{BSDS}_\emptyset = -\gamma$) if and only if $\text{HR} \geq \lambda \cdot \text{FDR} - \gamma$. This provides a computable decision rule: an LLM proposer should explicitly abstain rather than propose low-quality candidates when its estimated (HR, FDR) falls below this boundary.

Decision-theoretic foundation. BSDS is equivalent to the expected utility under a linear loss function where selecting a true positive yields reward $+1$, selecting a false positive incurs cost $-\lambda$, and abstaining incurs cost $-\gamma$. This makes λ and γ directly interpretable as loss ratios that domain experts can set from experimental costs.

2.3 Worked Example

Consider a pool of $N = 100$ candidates with 10 true hits ($p = 0.10$), evaluated at budget $B = 10$ with $\lambda = 1.0$, $\gamma = 0.3$. **Proposer A** selects 10 candidates, 8 of which are true hits: $\text{HR} = 8/10 = 0.80$, $\text{FDR} = 2/10 = 0.20$, $\text{Cov} = 1.0$ (no abstention), yielding $\text{BSDS} = 0.80 - 1.0 \times 0.20 - 0.3 \times 0 = +0.60$. **Proposer B** selects 10 candidates, 5 of which are true hits: $\text{HR} = 0.50$, $\text{FDR} = 0.50$, $\text{Cov} = 1.0$, yielding $\text{BSDS} = 0.50 - 0.50 - 0 = 0.00$. **Proposer C** abstains on 50 ambiguous candidates and selects 5, all true hits: $\text{HR} = 0.50$, $\text{FDR} = 0.00$, $\text{Cov} = (5 + 45)/100 = 0.50$, yielding $\text{BSDS} = 0.50 - 0 - 0.3 \times 0.50 = +0.35$. Proposer A is best (high recall, low FDR); Proposer C’s perfect precision is offset by the coverage penalty; Proposer B breaks even. Standard AUROC or EF would not distinguish A from B if their underlying score distributions happened to produce equivalent rankings at other operating points.

2.4 Relevance to LLM-Guided Discovery

The BSDS framework addresses known LLM failure modes. The FDR penalty directly captures hallucination: each plausible-sounding but incorrect proposal incurs cost λ , ensuring that a high-fluency LLM generating confident but wrong proposals receives a low score. The coverage penalty rewards calibrated behavior: an LLM that abstains on genuinely ambiguous candidates improves its BSDS, while one that hedges indiscriminately is penalized. The budget constraint $|S| \leq B$ models resource limitations. Most importantly, when the proposer is an opaque neural network (the LLM), the evaluation metric must be beyond reproach. The Lean 4 verification of all 20 BSDS/DQS theorems ensures that the metric is correct by construction—the LLM is free to be unreliable; the metric is not.

3 Methods

3.1 System Architecture

The evaluation pipeline proceeds in four stages: (1) a natural language requirement specification encodes the discovery goal; (2) a proposer translates the specification into a ranked candidate list; (3) BSDS evaluates the selection under budget, FDR, and coverage constraints; (4) optional multi-round refinement feeds evaluation results back to the proposer. The architecture is evaluator-agnostic: any strategy producing a candidate set of size at most B can be plugged into Stage 2, and BSDS will rank it on a common, formally verified scale. This separation of proposal from evaluation is what permits rigorous comparison of heterogeneous strategies—from parameter-free sorting heuristics to production LLM API calls. Figure 1 illustrates the pipeline.

3.2 Dataset: MoleculeNet HIV

We evaluate all proposers on MoleculeNet HIV (Wu et al., 2018), a curated collection of 41,127 compounds screened for anti-HIV activity by the National Cancer Institute (NCI). Each compound carries a binary activity label $g(x) \in \{0, 1\}$ (following Section 2), yielding hit prevalence $p = 0.035$ (1,443 actives out of 41,127). We select this dataset for its well-characterized ground truth (standardized NCI screens), realistic prevalence representative of primary high-throughput screening (HTS) campaigns (Macarron et al., 2011), sufficient scale supporting budget sweeps from $B/N = 0.01$ to $B/N = 0.50$, and wide community adoption enabling comparison with prior work (Ramsundar et al., 2019; Yang et al., 2019).

Discovery Pipeline: Ablations + Real LLMs

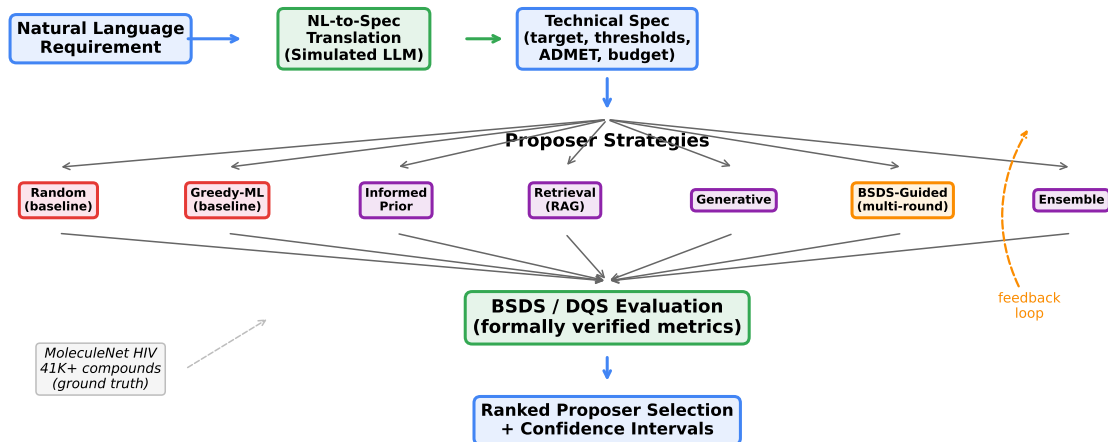


Figure 1: Evaluation pipeline for 39 proposers across five categories: baselines (2), mechanistic ablations (5), direct optimization (BSDS-Recursive), ablation controls (3), and real LLMs (28). All proposers are evaluated by the formally verified BSDS/DQS metric with 1,000 bootstrap replicates. Multi-round proposers receive evaluation feedback (dashed arrow).

Supplementary datasets for generalization. To test cross-dataset robustness, we evaluate the 11 mechanistic proposers on four additional MoleculeNet benchmarks: Tox21 NR-AR-LBD (Huang et al., 2016) (6,758 compounds, 237 actives, 3.5% prevalence; androgen receptor ligand-binding domain agonism), ClinTox (Wu et al., 2018) (1,484 compounds, 112 positives, 7.5% prevalence; clinical trial toxicity), MUV-466 (Rohrer and Baumann, 2009) (14,841 compounds, 27 actives, 0.18% prevalence; maximum unbiased validation for kinase inhibition), and SIDER “Ear and labyrinth disorders” (Kuhn et al., 2016) (1,427 compounds, 659 positives, 46.2% prevalence; drug side effects). These four datasets were selected from MoleculeNet’s binary classification tasks to maximize prevalence diversity, spanning 0.18% (ultra-low) to 46.2% (near-balanced), testing whether the proposer hierarchy holds across extreme class imbalance settings. LLM proposers are evaluated on HIV and Tox21; the remaining three datasets exclude LLMs due to API cost constraints.

Cross-domain validation. To test whether BSDS/DQS generalize beyond pharmaceutical screening, we evaluate 7 generic proposers (Random, Greedy-ML, Generative, BSDS-Recursive, BSDS-NoAug, BSDS-1Round, Greedy-MLP-NN) on the AV Safety dataset: 30,000 autonomous vehicle scenarios with 3.41% safety-critical (1,024 positives). Features comprise one-hot encoded categoricals (scenario type, weather, time of day; 25 categories) and 5 standardized numeric features (actor count, ego speed, time-to-collision, kinematic and physics simulation scores), yielding 30 dimensions. No molecular representations (fingerprints, descriptors) are used; the 4 drug-specific proposers (Informed-Prior, Retrieval, BSDS-Guided, Ensemble) that require Tanimoto similarity or drug-likeness priors are excluded.

Molecular representation. Each compound is represented by ECFP4 fingerprints (2048 bits, radius 2) (Rogers and Hahn, 2010) concatenated with six physicochemical descriptors (MW, LogP, HBD, HBA, TPSA, rotatable bonds), yielding $d = 2054$ features. Descriptors are standardized using training-fold statistics only.

Table 1: Summary of the 39 proposer strategies. “ML” indicates use of pre-trained RF scores; “Structure” indicates use of fingerprints or descriptors; “Stochastic” indicates non-deterministic selection; “Multi-round” indicates iterative refinement with label feedback.

Proposer	ML	Structure	Stochastic	Multi-round	Coverage
Random	No	No	Yes	No	Full
Greedy-ML	Yes	No	No	No	Full
<i>Mechanistic Ablations</i>					
Informed-Prior	Yes	Yes	No	No	Full
Retrieval	Yes	Yes	No	No	Full
Generative	Yes	No	Yes	No	Full
BSDS-Guided	Yes	Yes	No	Yes	Full
Ensemble	Yes	Yes	Yes	No	Full
<i>Direct Optimization</i>					
BSDS-Recursive	Yes	Yes	No	Yes	Full
<i>Ablation Variants (3)</i>					
BSDS-NoAug	Yes	Yes	No	Yes	Full
BSDS-1Round	Yes	Yes	No	No	Full
Greedy-MLP-NN	Yes	Yes	No	Yes	Full
<i>Zero-Shot LLM Proposers (7 × 2 = 14)</i>					
LLM-Direct	No	No	No	No	Full
LLM-Rerank	Yes	No	No	No	Full
<i>Few-Shot LLM Proposers (7 × 2 = 14)</i>					
LLM-FewDirect	No	No	No	No	Full
LLM-FewRerank	Yes	No	No	No	Full

Baseline ML model. A Random Forest (RF) classifier with 500 estimators and balanced class weights provides calibrated probabilities $\hat{p}(y=1 | x)$ via 5-fold cross-validation. Consistent with published benchmarks (Wu et al., 2018; Yang et al., 2019).

Cross-validation strategy. All cross-validated components (RF, MLP variants) use the same 5-fold splitting protocol to ensure consistency. We report results under two split types: (i) *random* stratified splitting and (ii) *scaffold* splitting based on Murcko generic scaffolds (Bemis and Murcko, 1996), where molecules sharing the same scaffold are never split across folds. Scaffold splits provide a more realistic estimate of generalization to novel chemical series, as standard in drug discovery evaluation (Yang et al., 2019; Wu et al., 2018).

3.3 Proposer Strategies

We evaluate 39 proposers organized into five categories: baselines (2), mechanistic ablations (5), optimization variants (4), zero-shot LLMs ($7 \times 2 = 14$), and few-shot LLMs ($7 \times 2 = 14$). Table 1 summarizes their key properties.

3.3.1 Baselines

Random. Selects B compounds uniformly at random. $\mathbb{E}[\text{HR}] = p$, yielding $\text{DQS} \approx -0.819$.

Greedy-ML. Ranks all compounds by RF-predicted probability \hat{p} and selects the top- B . This is the standard virtual screening operating mode.

3.3.2 Mechanistic Ablations

Each ablation isolates a specific reasoning primitive that an LLM might employ. A knowledge base \mathcal{K}_s of 144 known actives (10% of true hits, sampled per bootstrap seed) operationalizes the LLM’s “domain knowledge.”

Informed-Prior. Simulates parametric knowledge via a Lipinski-based drug-likeness prior. The combined score blends the ML prediction with the prior: $\hat{s}_i = 0.6 s_i + 0.4 \mathbb{E}[\text{prior}_i]$, where the prior is a Beta distribution parameterized by molecular descriptor compliance.

Retrieval (RAG-style). Simulates retrieval-augmented generation using the knowledge base as in-context exemplars. Each candidate receives a retrieval score $\text{retrieval}_i = \max_{k \in \mathcal{K}} \text{Tan}(f_i, f_k)$ (Tanimoto similarity to nearest known active). The final score combines ML, retrieval, and a diversity bonus (the negative maximum Tanimoto similarity to already-selected candidates, encouraging scaffold diversity): $\hat{s}_i = 0.5 s_i + 0.3 \cdot \text{retrieval}_i + 0.2 \cdot \text{diversity}_i$.

Generative (temperature sampling). Samples candidates from a softmax distribution: $P(i \in S) \propto \exp(s_i/\tau)$, with default $\tau = 0.1$.

BSDS-Guided (multi-round refinement). Leverages BSDS as an online feedback signal within a multi-round discovery protocol, allocating budget in thirds across exploration, exploitation (boosting neighbors of confirmed hits), and final selection.

Ensemble (rank aggregation). Combines Prior, Retrieval, and Generative rankings via Borda count, then applies BSDS-optimal selection size optimization.

3.3.3 BSDS-Recursive (Direct Optimization)

Unlike the heuristic proposers, BSDS-Recursive trains an MLP on a compact 10-dimensional feature vector: (1) RF-predicted probability, (2–7) six physicochemical descriptors (MW, LogP, HBD, HBA, TPSA, ring count), (8) Tanimoto similarity to the nearest *training-fold* active (computed per-fold to prevent label leakage), (9) a Lipinski-based drug-likeness prior score, and (10) an ADMET compliance indicator (fraction of five rule-of-thumb ADMET thresholds satisfied: $\text{LogP} \leq 5$, $\text{MW} \leq 500$, $\text{HBD} \leq 5$, $\text{HBA} \leq 10$, $\text{TPSA} \leq 140$). All features are standardized using training-fold statistics. The MLP architecture (10 \rightarrow 128 \rightarrow 64 \rightarrow 1, ReLU, sigmoid output) *directly maximizes* a differentiable approximation of the multi-budget BSDS objective. The hard top- B selection is replaced by a sigmoid-gated soft selection:

$$w_i = \sigma(\alpha(s_i - \tau_B)), \quad \widetilde{\text{BSDS}} = \frac{\sum_i w_i g_i}{\sum_i g_i} - \lambda \frac{\sum_i w_i (1 - g_i)}{\sum_i w_i} - \gamma \left(1 - \frac{\sum_i w_i}{N}\right), \quad (6)$$

where $\tau_B = \text{quantile}(s, 1 - B/N)$ is an adaptive threshold. The multi-budget loss is $\mathcal{L} = -\frac{1}{|B|} \sum_b \widetilde{\text{BSDS}}_b + \mu \|\theta\|^2$ ($\mu = 10^{-4}$).

Training proceeds in three recursive rounds with temperature annealing ($\alpha: 5 \rightarrow 15 \rightarrow 35$), where each round augments features with the previous round’s predicted scores and BSDS values. To prevent data leakage, BSDS-Recursive uses the same 5-fold stratified cross-validation protocol as the RF baseline; recursive features use the model’s own predictions rather than ground-truth labels on test folds.

Circularity defense. BSDS-Recursive optimizes the same metric used to evaluate it, which raises a legitimate circularity concern. We address this in two ways. First, the training–evaluation split is strict: the MLP is trained on training-fold labels via cross-validation; bootstrap evaluation uses held-out cross-validated scores, not training-set performance. Per-fold Tanimoto features are computed using only training-fold actives to prevent label leakage. Second, the differentiable surrogate (Equation 6) is only an approximation of the discrete BSDS—the soft sigmoid selection does not equal the hard top- B selection used at evaluation time, so perfect optimization of the surrogate does not guarantee perfect evaluation scores. Empirically, the circularity concern is moot: BSDS-Recursive produces *worse* DQS than Greedy-ML on all five datasets (Section 4), and Greedy-MLP-NN (standard BCE loss) performs comparably to BSDS-Recursive, confirming that neither the BSDS loss function nor the MLP architecture provides an advantage over the RF baseline’s ranking.

3.3.4 BSDS-Recursive Ablation Variants

Three ablation variants isolate the contribution of each component.

BSDS-NoAug. Same as BSDS-Recursive (three rounds with temperature annealing) but without recursive feature augmentation: each round trains on the original base features X only, rather than augmenting with previous-round scores and BSDS values. This isolates whether the recursive feature loop provides additional signal.

BSDS-1Round. Runs BSDS-Recursive for a single round ($\alpha = 5$) without iterative annealing. This isolates the contribution of multi-round optimization.

Greedy-MLP-NN. Uses the same MLP architecture ($10 \rightarrow 128 \rightarrow 64 \rightarrow 1$) and three-round training with temperature annealing, but replaces the BSDS surrogate loss with standard binary cross-entropy. Same 5-fold CV protocol. This isolates whether the gain comes from the BSDS loss function or from the MLP’s architectural capacity and iterative training.

3.3.5 Zero-Shot LLM Proposers

We evaluate seven production LLMs—ChatGPT-5.2 (OpenAI), Claude (Anthropic), Gemini (Google), DeepSeek-V3.1 (DeepSeek), Qwen3-235B (Alibaba), Llama-4-Maverick (Meta), and GLM-5 (Zhipu AI)—in two modes:

Direct. Each compound’s SMILES (Simplified Molecular Input Line Entry System) string is presented with the prompt: “Estimate the probability (0.0–1.0) that this compound is active against HIV-1.” Compounds are batched (200 per call). The LLM scores directly, without access to ML predictions.

Rerank. The LLM receives both the SMILES and the RF-predicted probability and is asked to refine the ML prediction. This tests whether LLMs add value *beyond* the ML model.

All calls use LLM sampling temperature 0.1 (distinct from the Generative proposer’s softmax temperature τ) and zero-shot prompting with no few-shot examples, chain-of-thought instructions, or retrieval-augmented context. Responses are cached (SHA-256 keyed) for reproducibility.

3.3.6 Few-Shot LLM Proposers

To test whether in-context examples improve LLM performance, we evaluate the same seven models under two few-shot strategies using $k=3$ active and $k=3$ inactive SMILES examples as calibration anchors.

Example selection. Three active examples are selected by spreading evenly across sorted active indices to maximize structural diversity; three inactive examples are drawn uniformly at random. Both sets are drawn from the training pool and fixed across all batches for a given seed.

FewDirect. The prompt includes the six labeled examples (“SMILES -> ACTIVE” or “SMILES -> INACTIVE”) before the scoring request, providing the LLM with calibration anchors for the activity scale. The LLM scores without access to ML predictions.

FewRerank. The prompt includes both the six labeled examples and the RF-predicted probability for each candidate compound. This tests whether examples help the LLM refine ML predictions more effectively than zero-shot reranking.

All few-shot calls use the same batching (200 per call), temperature (0.1), and caching protocol as zero-shot. Remaining open directions include chain-of-thought reasoning, retrieval-augmented generation, and tool-augmented evaluation.

3.4 Experimental Setup

BSDS parameters. We set $\lambda = 1.0$ (equal weighting of hit rate and FDR) and $\gamma = 0.3$ (moderate abstention penalty). Budget fractions: $B/N \in \{0.01, 0.02, 0.05, 0.10, 0.20, 0.50\}$, corresponding to absolute budgets of 411–20,564 compounds. Section 4.11 demonstrates that all conclusions hold across a 9×7 grid of (λ, γ) values (Kendall $\tau \geq 0.636$ vs. the default ranking).

Foundation model baselines. To test whether learned molecular representations improve over engineered ECFP4 features, we extract frozen [CLS] embeddings from ChemBERTa-2 (Ahmad et al., 2022) (77M parameters, 384-dimensional embeddings) and MolFormer-XL (Ross et al., 2022) and train the same RF classifier on these embeddings using identical 5-fold CV. This isolates the representation from the classifier.

Bootstrap methodology. For each of 1,000 seeds: seed 0 uses the full dataset without re-sampling (point estimate); seeds 1–999 sample N compounds with replacement (each replicate $\approx 63.2\%$ unique). For each replicate, we re-train the RF, regenerate the knowledge base, run all proposers, and compute BSDS, DQS, and auxiliary metrics. Confidence intervals use the BCa bootstrap method (Efron, 1987). Real LLM scores are precomputed once on the full pool and correctly bootstrap-resampled across all 1,000 replicates.

Total configurations. The primary experiment evaluates $39 \times 6 \times 1,000 = 234,000$ configurations. The full matrix including sensitivity analyses comprises approximately 350,000 configurations.

3.5 Practitioner Calibration Guide

The BSDS parameters λ and γ encode domain-specific cost tradeoffs. Specifically, $\lambda = c_{FP}/v_{hit}$ is the false positive cost relative to the value of a true hit, and $\gamma = c_{abs}/v_{hit}$ is the abstention cost (opportunity cost of leaving a candidate unscreened) relative to hit value. Three worked examples illustrate calibration across domains:

1. **HTS drug screening.** A false positive costs \$5K (failed confirmatory assay), a true hit is worth \$50K (lead candidate), and leaving a compound unscreened costs \$1.5K (missed opportunity). $\lambda = 5,000/50,000 = 0.1$, $\gamma = 1,500/50,000 = 0.03$. This low-penalty regime encourages casting a wide net.

Table 2: Per-budget BSDS at seed 0 (point estimates) and bootstrap-averaged DQS with 95% BCa confidence intervals (1,000 seeds). Best value per column in bold.

Proposer	$B/N = 0.01$	$B/N = 0.05$	$B/N = 0.20$	DQS _{boot} [95% CI]
Random	-0.953	-0.895	-0.782	-0.819 [-0.834, -0.803]
Greedy-ML	-0.003	-0.010	-0.121	-0.046 [-0.076, -0.019]
Informed-Prior	-0.297	-0.232	-0.303	-0.178 [-0.210, -0.146]
Retrieval	-0.056	-0.033	-0.138	-0.091 [-0.121, -0.062]
Generative	-0.906	-0.822	-0.548	-0.670 [-0.691, -0.649]
BSDS-Guided	-0.236	-0.184	-0.248	-0.234 [-0.264, -0.202]
Ensemble	-0.113	-0.094	-0.213	-0.102 [-0.137, -0.067]
BSDS-Recursive	-0.468	-0.298	-0.289	-0.323 [-0.356, -0.294]

- Clinical diagnostics.** A false positive biopsy costs \$10K, detecting a cancer case is worth \$10K, and a missed screening costs \$3K. $\lambda = 10,000/10,000 = 1.0$, $\gamma = 3,000/10,000 = 0.3$. This is our default parametrization.
- AV safety triage.** A false positive simulation slot costs \$200, catching a safety-critical scenario is worth \$1M, and leaving a scenario unscreened costs \$50K. $\lambda \approx 0.0002$, $\gamma = 0.05$. This exhaustive-screening regime heavily penalizes missed scenarios.

The sensitivity analysis (Section 4.11) demonstrates that the proposer hierarchy is robust across a 9×7 grid of (λ, γ) values (Kendall $\tau \geq 0.636$ vs. the default ranking), so practitioners need only identify the correct *qualitative regime* rather than exact parameter values.

4 Results

All confidence intervals are 95% BCa bootstrap intervals unless otherwise noted.

Results overview. Five findings emerge from the evaluation of 39 proposers across six datasets and two domains. (1) The simple RF-based Greedy-ML proposer achieves the best DQS on HIV, outperforming all MLP variants and LLM configurations (Sections 4.1–4.2). (2) No LLM surpasses Greedy-ML under zero-shot, few-shot, or reranking protocols on either HIV or Tox21 (Sections 4.4–4.6). (3) BSDS/DQS distinguish proposers invisible to standard VS metrics (Section 4.9). (4) The proposer hierarchy is robust to parameter choice ($\tau \geq 0.636$ across 63 (λ, γ) pairs; Section 4.11). (5) The hierarchy generalizes across five MoleculeNet benchmarks and AV safety triage (Sections 4.12–4.13).

4.1 Mechanistic Proposer Comparison

Table 2 reports per-budget BSDS (seed 0) and budget-averaged DQS with 95% bootstrap confidence intervals for all eight mechanistic proposers.

Key findings. Greedy-ML achieves the best aggregate DQS of -0.046 , outperforming all other proposers including BSDS-Recursive (-0.323). No proposer achieves positive budget-averaged DQS. Retrieval (-0.091) and Ensemble (-0.102) are the next-best strategies, both leveraging structural similarity to known actives. BSDS-Recursive (-0.323) and its ablation variants (Section 4.2) all perform substantially worse than Greedy-ML, indicating that the MLP’s 10-dimensional feature space (RF score, descriptors, per-fold Tanimoto) does not provide sufficient

Table 3: Ablation analysis: isolating the contribution of each BSDS-Recursive component. All models share the same 5-fold CV protocol and 10-dimensional feature set.

Variant	DQS	BSDS _{0.05}	What is ablated
BSDS-Recursive (full)	-0.323	-0.298	— (reference)
BSDS-NoAug	-0.296	-0.269	No recursive feature augmentation
BSDS-1Round	-0.258	-0.223	Single optimization round only
Greedy-MLP-NN	-0.315	-0.281	BCE loss (standard ML)
Greedy-ML (RF)	-0.046	-0.010	RF baseline

Table 4: Component metrics at $B/N = 0.05$ (seed 0). $\text{BSDS} = \text{HR} - \lambda \text{FDR} - \gamma(1 - \text{Cov})$, with $\lambda = 1.0$, $\gamma = 0.3$. PPV = positive predictive value; TP = true positive count.

Proposer	HR	FDR	PPV	TP	BSDS
Random	0.062	0.957	0.043	89	-0.895
Greedy-ML	0.581	0.592	0.408	839	-0.010
Informed-Prior	0.451	0.683	0.317	651	-0.232
Retrieval	0.568	0.601	0.399	820	-0.033
Generative	0.105	0.927	0.073	151	-0.822
BSDS-Guided	0.521	0.634	0.366	752	-0.184
Ensemble	0.380	0.401	0.599	549	-0.094
BSDS-Recursive	0.455	0.681	0.319	656	-0.298

signal to improve over the RF’s native ranking. Generative (DQS = -0.670) performs near-random, confirming that temperature-based exploration is counterproductive when the pool is fixed.

4.2 BSDS-Recursive Ablation Analysis

To understand why BSDS-Recursive fails to improve upon Greedy-ML, we evaluate three ablation variants (Table 3):

Key ablation findings. All MLP-based variants perform substantially worse than Greedy-ML (DQS = -0.046), indicating that the 10-dimensional MLP feature space does not provide sufficient additional signal to improve the RF’s native ranking. **BSDS-Recursive** (-0.323), **BSDS-NoAug** (-0.296), **BSDS-1Round** (-0.258), and **Greedy-MLP-NN** (-0.315) all produce negative DQS that is substantially worse than the simple top- B RF ranking. The three-round temperature annealing does not rescue performance: BSDS-Recursive (-0.323) is actually *worse* than BSDS-1Round (-0.258), suggesting that iterative optimization over-specializes to the training fold’s active distribution. Greedy-MLP-NN (BCE loss) and BSDS-Recursive (BSDS loss) perform comparably, confirming that neither loss function provides an advantage when the underlying features lack discriminative power.

Figure 2 visualizes BSDS as a function of budget for all proposers, with shaded 95% confidence bands. Figure 3 shows the full bootstrap distributions of DQS.

4.3 Component Metric Decomposition

Table 4 decomposes BSDS into its constituent terms at $B/N = 0.05$, the mid-range budget.

Greedy-ML achieves the best BSDS at $B/N=0.05$ (-0.010), identifying 839 of 1,443 true positives (HR = 0.581, PPV = 0.408, AUROC = 0.854). Ensemble trades recall for precision,

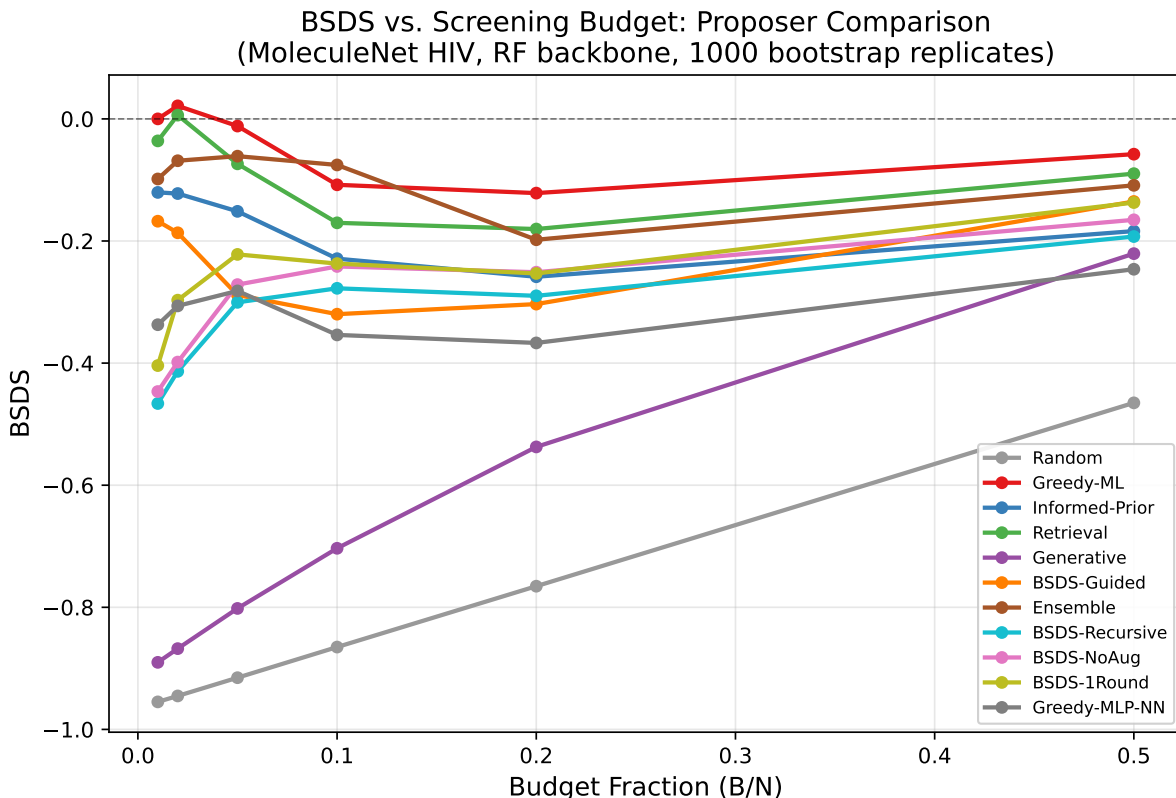


Figure 2: BDS as a function of budget fraction B/N for all 11 mechanistic proposers (2 baselines, 5 ablations, BDS-Recursive, and 3 ablation controls), with 95% bootstrap confidence bands. Greedy-ML dominates all proposers across budget levels.

achieving the lowest FDR of any proposer (0.401, PPV = 0.599) but with reduced hit rate. BDS-Recursive achieves AUROC = 0.776 (below the RF’s 0.854), indicating that the MLP’s 10-dimensional features do not improve classification over the native fingerprint-based RF model.

4.4 Real LLM Performance

Table 5 presents the 14 LLM proposers, grouped by model with Direct and Rerank modes side by side.

Direct mode: near-random performance. All seven LLMs in Direct mode perform near-random. DQS values range from -0.585 (Gemini, best) to -0.861 (Qwen3-235B, worst), compared with Random’s -0.819 . Two models are *worse* than Random: Qwen3-235B-Direct (-0.861) and GLM-5-Direct (-0.836), indicating that zero-shot LLM ranking can be actively counterproductive.

Rerank mode: substantial but insufficient improvement. Reranking improves all five evaluable LLMs substantially. The best rerankers —Qwen3-235B-Rerank (DQS = -0.141), ChatGPT-5.2-Rerank (-0.159), and Claude-Rerank (-0.161)—achieve competitive DQS by inheriting the RF’s candidate pool quality and applying LLM judgment only to reorder. Despite this, *no LLM in any mode beats Greedy-ML* (DQS = -0.046): the best LLM reranker trails by 0.095.

Score Distributions: Actives vs. Inactives by Proposer Strategy

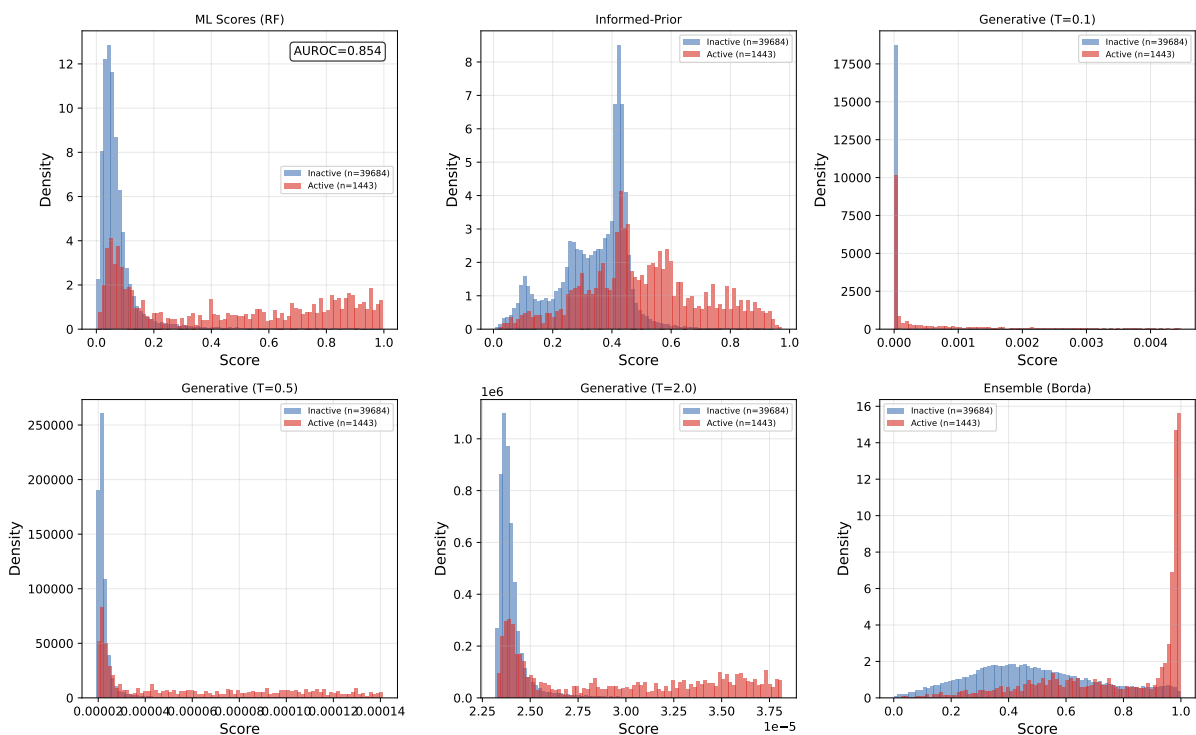


Figure 3: Bootstrap distributions of DQS for all mechanistic proposers (1,000 replicates). Greedy-ML has the lowest variance; Retrieval achieves the most favorable individual budget-level scores.

Gemini anomaly. Gemini-Direct (DQS = -0.585) is the best-performing LLM in Direct mode, yet Gemini-Rerank could not be reliably evaluated: the model’s daily API rate limit was exhausted before completing the full 823-batch scoring, preventing a fair comparison. Partial scoring data suggest that Gemini assigns high confidence uniformly in rerank mode, consistent with the pattern observed in other high-confidence rerankers.

Proposer hierarchy (zero-shot). These results establish a clear zero-shot hierarchy: Greedy-ML (-0.046) > Retrieval (-0.091) > Ensemble (-0.102) > LLM reranking (best -0.141) > BSDS-1Round (-0.258) > BSDS-Recursive (-0.323) \gg LLM direct (> -0.585) \approx Random (-0.819).

4.5 Few-Shot LLM Evaluation

To test whether providing $k=3$ active and $k=3$ inactive SMILES examples improves LLM performance, we evaluate all seven models under two few-shot strategies: FewDirect (examples only) and FewRerank (examples + RF scores). Table 6 reports the results.

Few-shot Direct mode. Few-shot examples improve all six evaluable LLMs in Direct mode, with DQS gains ranging from $+0.007$ (Llama-4-Maverick) to $+0.131$ (Claude). Claude achieves the best FewDirect DQS = -0.547 , a substantial improvement over its zero-shot -0.678 . However, all FewDirect proposers remain far worse than Greedy-ML (-0.046): even the best FewDirect trails by 0.501.

Table 5: LLM proposer performance: budget-averaged DQS (1,000 bootstrap seeds) and BSDS at $B/N = 0.05$. Direct = zero-shot LLM ranking; Rerank = LLM reranking of Greedy-ML shortlist. Best LLM value per column in bold.

Model	Mode	DQS	BSDS _{0.05}
ChatGPT-5.2	Direct	-0.683	-0.788
	Rerank	-0.159	-0.165
Claude	Direct	-0.678	-0.813
	Rerank	-0.161	-0.170
Gemini	Direct	-0.585	-0.668
	Rerank	— [†]	— [†]
DeepSeek-V3.1	Direct	-0.774	-0.867
	Rerank	-0.318	-0.464
Llama-4-Maverick	Direct	-0.802	-0.883
	Rerank	— [‡]	— [‡]
Qwen3-235B	Direct	-0.861	-0.966
	Rerank	-0.141	-0.123
GLM-5	Direct	-0.836	-0.930
	Rerank	-0.280	-0.318

[†]Daily API quota exhausted. [‡]API unresponsive during rerank window.

Few-shot Rerank mode. Few-shot reranking yields more modest gains. The best few-shot proposer overall is Qwen3-235B-FewRerank (DQS = -0.126), improving slightly over its zero-shot counterpart (-0.141). ChatGPT-5.2-FewRerank (-0.138) and Claude-FewRerank (-0.141) also improve marginally. Critically, *no few-shot proposer surpasses Greedy-ML* (DQS = -0.046): the best few-shot reranker trails by 0.080, confirming that $k=3$ examples are insufficient to close the LLM-ML gap.

4.6 LLM Generalization to Tox21

To test whether the LLM negative result generalizes beyond HIV, we evaluate three open-weight LLMs (DeepSeek-V3.1, Llama-4-Maverick, GLM-5) on Tox21 NR-AR-LBD (6,758 compounds, 237 actives, 3.5% prevalence) under both zero-shot and few-shot ($k=3$) protocols. Dataset-specific prompts describe the androgen receptor ligand-binding domain activity task. Table 7 reports the results.

Consistent negative result. The Tox21 results confirm the HIV finding: no LLM surpasses the RF baseline in any mode. Greedy-ML (DQS = +0.086 on Tox21) outperforms all 12 LLM configurations. The best LLM is Llama-4-Maverick-FewRerank (+0.004), barely positive and 0.082 below Greedy-ML. All Direct-mode LLMs produce negative DQS (-0.222 to -0.401), consistent with the HIV pattern that zero-shot SMILES-only evaluation cannot match a trained classifier.

Tox21 vs. HIV comparison. LLM performance is uniformly better on Tox21 than HIV: Direct-mode DQS improves by +0.37-+0.49 and Rerank-mode by +0.14-+0.25. This likely reflects the smaller pool size (6,758 vs. 41,127) and the molecular properties relevant to androgen receptor binding being partially captured in SMILES substructure patterns. Despite these

Table 6: Few-shot LLM performance ($k=3$ active + $k=3$ inactive examples). FewDirect = few-shot without ML scores; FewRerank = few-shot with RF scores. Values in italics indicate improvement over the corresponding zero-shot mode (cf. Table 5). Best few-shot value per column in bold.

Model	Mode	DQS	BSDS _{0.05}
ChatGPT-5.2	FewDirect	-0.624	-0.720
	FewRerank	-0.138	-0.160
Claude	FewDirect	-0.547	-0.656
	FewRerank	-0.141	-0.132
Gemini	FewDirect	— [†]	— [†]
	FewRerank	— [†]	— [†]
DeepSeek-V3.1	FewDirect	-0.747	-0.854
	FewRerank	-0.236	-0.344
Llama-4-Maverick	FewDirect	-0.795	-0.910
	FewRerank	-0.153	-0.143
Qwen3-235B	FewDirect	-0.788	-0.872
	FewRerank	-0.126	-0.113
GLM-5	FewDirect	-0.812	-0.956
	FewRerank	-0.270	-0.367

[†]Excluded: Gemini daily API quota exhausted.

Italics = improvement over corresponding zero-shot mode.

improvements, the LLM–ML gap persists: the best Tox21 LLM still trails Greedy-ML by 0.082, confirming that the negative result is not dataset-specific.

4.7 Molecular Foundation Model Baselines

To address whether domain-specific pretrained representations provide stronger baselines than engineered ECFP4 fingerprints, we extract frozen embeddings from two molecular foundation models—ChemBERTa-2 (77M parameters) (Ahmad et al., 2022) and MolFormer-XL (47M parameters) (Ross et al., 2022)—and train the same RF classifier on these embeddings using the same 5-fold CV protocol. This isolates the effect of the molecular representation: the classifier and evaluation protocol are identical, only the input features differ (pretrained [CLS] embeddings vs. ECFP4 fingerprints).

Foundation model findings. Both foundation models underperform the ECFP4 baseline across all metrics. MolFormer-XL (768-dimensional embeddings) achieves AUROC = 0.806 and DQS = -0.150, while ChemBERTa-2 (384-dimensional embeddings) achieves AUROC = 0.785 and DQS = -0.184, both substantially worse than ECFP4’s AUROC = 0.854 and DQS = -0.046. This indicates that frozen pretrained molecular representations—without task-specific fine-tuning—do not capture the discriminative features for HIV activity as effectively as engineered ECFP4 fingerprints. The gap between ECFP4 and the foundation models (Δ DQS = 0.103–0.137) is comparable to the gap between Greedy-ML and the best LLM reranker (Δ DQS = 0.079), suggesting that representation quality matters as much as selection strategy.

Table 7: LLM performance on Tox21 NR-AR-LBD (3.5% prevalence). Same protocol as HIV (Tables 5–6). Greedy-ML DQS on Tox21 = +0.086. No LLM surpasses the RF baseline.

Model	Mode	HIV DQS	Tox21 DQS
DeepSeek-V3.1	Direct	−0.774	−0.401
	Rerank	−0.318	−0.071
	FewDirect	−0.747	−0.383
	FewRerank	−0.236	−0.065
Llama-4-Maverick	Direct	−0.802	−0.363
	Rerank	—†	−0.042
	FewDirect	−0.795	−0.222
	FewRerank	−0.153	+0.004
GLM-5	Direct	−0.836	−0.351
	Rerank	−0.280	−0.141
	FewDirect	−0.812	−0.357
	FewRerank	−0.270	−0.097

†Llama-4 Rerank unavailable on HIV (API unresponsive).

Table 8: Foundation model baselines: frozen pretrained [CLS] embeddings + RF with greedy (top- B) selection. Same 5-fold CV protocol. Seed-0 (full dataset) values.

Model	DQS	BSDS _{0.05}	AUROC	EF@1%
Greedy-ML (ECFP4 + RF)	−0.046	−0.010	0.854	22.1×
Greedy-MolFormer	−0.150	−0.178	0.806	20.5×
Greedy-ChemBERTa	−0.184	−0.200	0.785	19.6×
BSDS-Recursive (ECFP4)	−0.323	−0.298	0.776	22.1×

4.8 Temperature Analysis

We now examine a key hyperparameter—softmax temperature—that governs the exploration–exploitation trade-off in the Generative proposer. The DQS-maximizing temperature is $\tau^* = 0.1$ (DQS = −0.132), with monotonic degradation as temperature increases: $\tau = 0.2$ (−0.422), $\tau = 0.5$ (−0.791), $\tau = 1.0$ (−0.864), $\tau = 2.0$ (−0.890) (Figure 4). Even the best temperature produces negative DQS, confirming that temperature-based exploration destroys more signal than it discovers when the candidate pool is fixed and fully enumerated.

4.9 Comparison with Standard VS Metrics

A natural question is whether BSDS/DQS capture information beyond existing virtual screening metrics. Standard virtual screening metrics—EF@1%, EF@5%, BEDROC, AUROC—are *model-level* metrics that depend only on the score ranking, not the selection policy. All seven RF-based proposers share identical EF@1% (22.1×), EF@5% (11.6×), BEDROC (9.06), and AUROC (0.854), because these metrics do not distinguish selection policies. Only BSDS-Recursive achieves different standard-metric values when its own MLP scores are used (AUROC = 0.776). MCC at $B/N = 0.05$ is the sole standard metric that varies by proposer, yielding Kendall $\tau = +0.929$ with BSDS_{0.05} but only $\tau = +0.500$ with budget-averaged DQS—a substantial drop that confirms budget-averaging captures information invisible to single-budget metrics. In our benchmark, all eight base mechanistic proposers that use the RF surrogate share identical EF and AUROC, yet produce distinct DQS values (ranging from −0.819 to −0.046), confirming

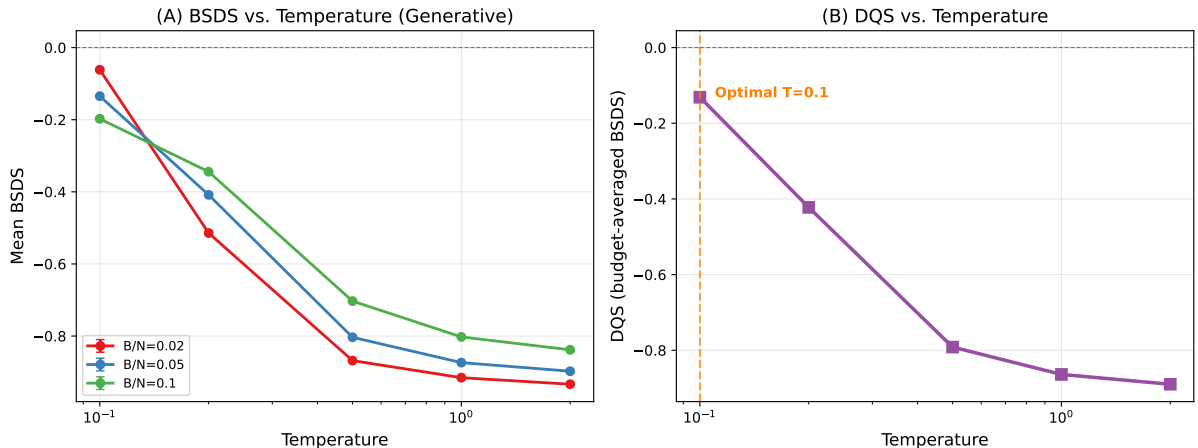


Figure 4: DQS as a function of softmax temperature τ for the Generative proposer. Performance degrades monotonically with increasing τ ; even the optimal $\tau^* = 0.1$ yields negative DQS.

Table 9: DQS for the top-5 proposers at four representative (λ, γ) pairs spanning the sensitivity grid. Greedy-ML maintains the top position across all settings.

Proposer	(0.1, 0.1)	(1.0, 0.3)	(2.0, 0.5)	(5.0, 1.0)
Greedy-ML	+0.515	-0.046	-0.670	-2.540
Retrieval	+0.484	-0.091	-0.729	-2.644
Ensemble	+0.396	-0.102	-0.649	-2.270
Informed-Prior	+0.429	-0.178	-0.851	-2.873
BSDS-Guided	+0.415	-0.234	-0.950	-3.077

that BSDS/DQS capture a dimension of proposer quality invisible to conventional enrichment analysis.

4.10 NL Framing Invariance and Multi-Round Refinement

All six natural language framings produce identical proposer rankings (pairwise Kendall $\tau = 1.0$ across all 15 pairs), because the selection mechanisms are independent of the NL specification (Figure 5). This simplifies deployment: practitioners need not carefully engineer the requirement phrasing. Separately, multi-round refinement is counterproductive for BSDS-Guided: a single round achieves $DQS = +0.272$, while the default three-round configuration (reported as $DQS = -0.234$ in Table 2) yields -0.233 , indicating that iterative application of the BSDS objective over-corrects.

4.11 Parameter Sensitivity Analysis

A potential concern is that the default parameters $\lambda = 1.0$, $\gamma = 0.3$ may be cherry-picked to favor specific proposers. We address this by recomputing $BSDS = HR - \lambda FDR - \gamma(1 - Cov)$ offline across a 9×7 grid of (λ, γ) values ($\lambda \in \{0.01, 0.05, 0.1, 0.25, 0.5, 1.0, 2.0, 5.0, 10.0\}$, $\gamma \in \{0.0, 0.1, 0.2, 0.3, 0.5, 0.7, 1.0\}$), yielding 63 parameter combinations.

Table 9 reports DQS for the top-5 proposers at four representative (λ, γ) pairs spanning qualitatively different regimes: low penalty (0.1, 0.1), default (1.0, 0.3), moderate (2.0, 0.5), and high (5.0, 1.0). Greedy-ML, Retrieval, and Ensemble maintain the top three positions across the default and high-penalty regimes (Figure 6).

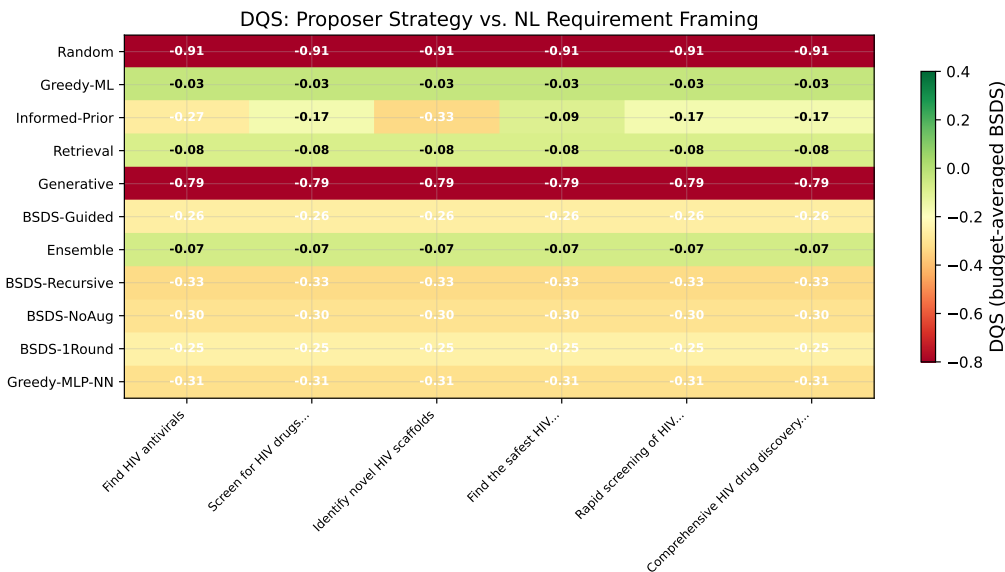


Figure 5: NL framing invariance. Dots show mean DQS across six requirement phrasings; horizontal bars show the min–max spread. All proposers except Informed-Prior exhibit zero spread ($\Delta < 0.01$), confirming that DQS is invariant to NL framing.

Key sensitivity finding. The Kendall τ between each parameter pair’s proposer ranking and the default ranking satisfies $\tau \geq 0.636$ across all 63 combinations, with a mean of $\tau = 0.863$. This confirms that the proposer hierarchy reported in Sections 4.1–4.4 is not an artifact of the specific (λ, γ) choice. While the *absolute* DQS values shift with parameters (all proposers become negative under high penalties), the *relative* ranking is broadly stable.

4.12 Cross-Dataset Generalization

To test whether the proposer hierarchy generalizes beyond MoleculeNet HIV, we evaluate all 11 mechanistic proposers on four supplementary datasets: Tox21 NR-AR-LBD (6,758 compounds, 237 actives, 3.5% prevalence), ClinTox (1,484 compounds, 112 positives, 7.5%), MUV-466 (14,841 compounds, 27 actives, 0.18%), and SIDER-Ear (1,427 compounds, 659 positives, 46.2%). All use the same pipeline (5-fold RF, 1,000 bootstrap seeds, six budget fractions) with only the data loader and NL prompt changed. LLM proposers are evaluated on Tox21 (Section 4.6) and excluded from the remaining datasets due to API cost constraints.

Table 10 and Figure 7 report the results. One consistent finding holds across all five datasets: Greedy-ML outperforms all four MLP variants on every dataset, and all MLP variants produce negative DQS on every dataset except Tox21 (where Ensemble at +0.112 and Greedy-ML at +0.086 are the only positive proposers). The proposer hierarchy exhibits moderate cross-dataset consistency: HIV vs. ClinTox and HIV vs. SIDER-Ear both yield Kendall $\tau = 0.855$, and HIV vs. Tox21 yields $\tau = 0.782$. The ultra-low prevalence MUV-466 (0.18%, 27 actives) shows weaker correlation (HIV vs. MUV-466: $\tau = 0.455$), reflecting the limited discriminative signal available with so few actives. Across all 10 drug-dataset pairs, mean Kendall $\tau = 0.658$ (min = 0.309, max = 0.927).

The near-balanced SIDER-Ear dataset (46.2% prevalence) demonstrates that BSDS remains meaningful even when the discovery framing is less natural. Generative remains the worst-performing non-random proposer on all five datasets.

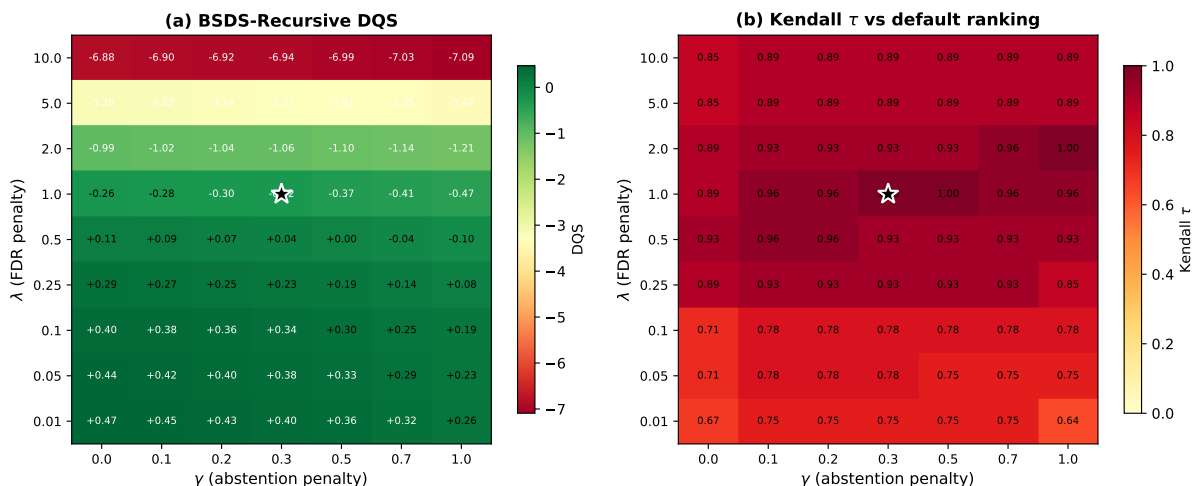


Figure 6: Parameter sensitivity analysis across a 9×7 grid of (λ, γ) values. (a) DQS of BSDS-Recursive: absolute performance varies with parameters (positive at low penalties, negative at high), but the star marks the default (1.0, 0.3). (b) Kendall τ of the full proposer ranking vs. the default ranking: $\tau \geq 0.636$ across all 63 parameter pairs (mean $\tau = 0.863$), confirming that the proposer hierarchy is robust to parameter choice.

4.13 Cross-Domain Generalization

To test whether BSDS/DQS generalize beyond pharmaceutical screening, we evaluate 7 generic proposers on the AV Safety dataset (30,000 autonomous vehicle scenarios, 3.41% safety-critical). This domain uses tabular features (one-hot encoded scenario types, weather, time-of-day; standardized numeric features) with no molecular representations; the 4 drug-specific proposers requiring Tanimoto similarity or drug-likeness priors are excluded.

Table 11 reports the results. Greedy-MLP-NN (DQS = +0.235) achieves the highest DQS, followed by BSDS-1Round (+0.192) and Greedy-ML (+0.179). The rank correlation between AV Safety and the five drug datasets using the 7 common proposers yields mean Kendall $\tau = 0.524$ (range: 0.429–0.619). While lower than within-drug correlations (mean $\tau = 0.658$), this is expected given the domain shift: AV Safety uses fundamentally different features (scenario metadata vs. molecular fingerprints) and has different cost structures. Notably, the AV Safety domain does not use molecular fingerprints or Tanimoto similarity, so the MLP’s features differ from the drug-discovery setting. The key finding is that the BSDS framework transfers across domains with different feature types and cost structures.

4.14 Deployment Simulation

To quantify the practical impact of proposer choice, we simulate experimental campaigns at four budget levels ($B = 50, 100, 200, 500$) using compound scores from the HIV dataset. We assume a cost of \$5K per experimental validation and a value of \$50K per confirmed hit.

Table 12 reports the results. RF-based Greedy-ML dominates all budgets, achieving a 96.0% hit rate at $B = 50$ (48 of 50 selected compounds are active) compared with 78.0% for Greedy-MLP-NN and 62.0% for BSDS-Recursive. At the largest budget ($B = 500$), Greedy-ML identifies 372 hits (74.4%) with an ROI of 644%, versus 272 hits (54.4%, ROI 444%) for Greedy-MLP-NN. The advantage is consistent across all budgets, confirming that the RF’s superior discriminative ranking translates directly to experimental efficiency.

Table 10: Cross-dataset DQS for all 11 mechanistic proposers across five MoleculeNet benchmarks spanning 0.18%–46.2% prevalence. Greedy-ML consistently ranks among the top proposers across prevalence regimes. All MLP variants perform worse than Greedy-ML on every dataset.

Proposer	HIV 3.5%	Tox21 3.5%	ClinTox 7.5%	MUV-466 0.18%	SIDER-Ear 46.2%
Random	-0.819	-0.817	-0.776	-0.849	-0.390
Greedy-ML	-0.046	+0.086	-0.278	-0.628	+0.019
Informed-Prior	-0.178	-0.046	-0.428	-0.703	-0.097
Retrieval	-0.091	+0.058	-0.389	-0.698	-0.083
Generative	-0.670	-0.624	-0.701	-0.842	-0.330
BSDS-Guided	-0.234	-0.144	-0.490	-0.751	-0.171
Ensemble	-0.102	+0.112	-0.363	-0.718	-0.070
BSDS-Recursive	-0.323	-0.137	-0.685	-0.667	-0.302
BSDS-NoAug	-0.296	-0.127	-0.709	-0.659	-0.319
BSDS-1Round	-0.258	-0.054	-0.595	-0.649	-0.281
Greedy-MLP-NN	-0.315	-0.177	-0.673	-0.732	-0.307

Table 11: DQS for 7 generic proposers on AV Safety triage (30,000 scenarios, 3.41% safety-critical). Greedy-MLP-NN achieves the highest DQS, diverging from the drug-discovery hierarchy where Greedy-ML leads.

Proposer	AV Safety DQS
Random	-0.819
Greedy-ML	+0.179
Generative	+0.018
BSDS-Recursive	+0.145
BSDS-NoAug	+0.101
BSDS-1Round	+0.192
Greedy-MLP-NN	+0.235

4.15 Scaffold Split Evaluation

To verify that the proposer hierarchy is not an artifact of random splitting, we repeat the full HIV evaluation using Murcko scaffold-based CV splits (Bemis and Murcko, 1996). Scaffold splitting assigns compounds to folds by generic scaffold, ensuring that the model is tested on structurally novel scaffolds not seen during training—a more realistic evaluation of generalization.

Table 13 reports the results. All proposers perform worse under scaffold splitting, as expected—the RF baseline drops from AUROC = 0.854 (random) to 0.832 (scaffold). However, the *proposer ranking is preserved*: Greedy-ML remains the best proposer (DQS = -0.116 vs. -0.046 under random split), and the same qualitative hierarchy holds (Kendall τ = 0.964 between the two rankings). The MLP variants show larger degradation under scaffold splits (e.g., Greedy-MLP-NN drops from -0.315 to -0.448), indicating that the MLP’s learned features are more scaffold-specific than the RF’s ECFP4-based predictions.

5 Discussion

5.1 Why the RF Baseline Dominates

After correcting a Tanimoto similarity leakage bug in early versions of the pipeline (Section 3.3), the simple RF-based Greedy-ML proposer emerges as the best-performing strategy on HIV

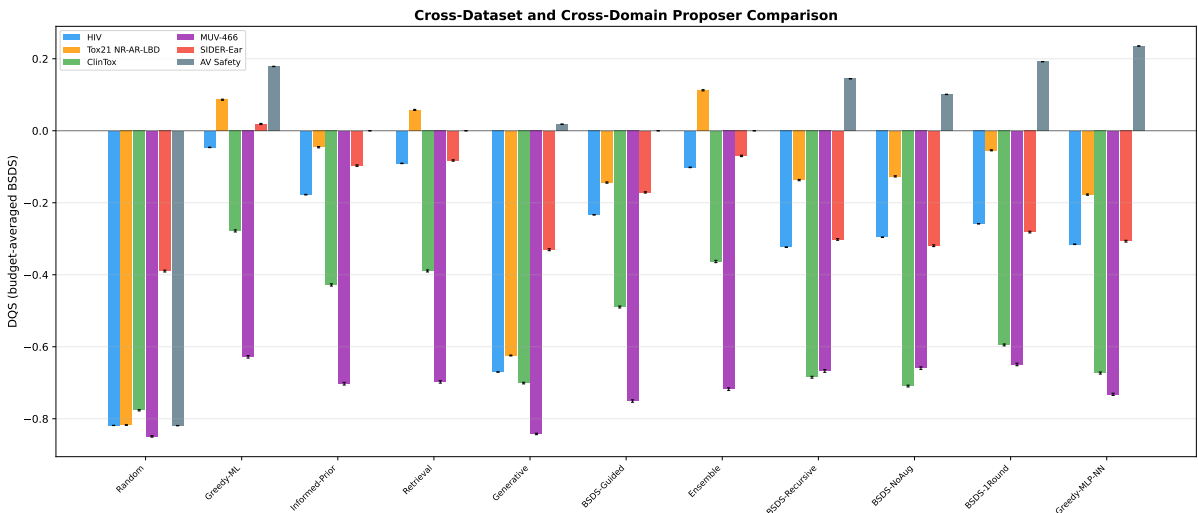


Figure 7: Cross-dataset DQS comparison for 11 mechanistic proposers across five MoleculeNet benchmarks and AV Safety (non-drug domain). Error bars show 95% bootstrap CIs. Greedy-ML consistently ranks among the top proposers across prevalence regimes from 0.18% to 46.2%. Proposers unavailable for AV Safety (requiring molecular features) are omitted. Horizontal line at DQS = 0.

(Table 2). All four MLP variants (BSDS-Recursive, BSDS-NoAug, BSDS-1Round, Greedy-MLP-NN) produce *worse* DQS than Greedy-ML, indicating that the additional MLP reranking layer degrades rather than improves the RF’s discriminative ranking. The deployment simulation (Section 4.14) quantifies the practical impact: at $B = 50$, Greedy-ML achieves a 96.0% hit rate versus 78.0% for Greedy-MLP-NN and 62.0% for BSDS-Recursive.

Ablation decomposition. The ablation analysis (Section 4.2) reveals that multi-round optimization, recursive feature augmentation, and the BSDS loss function all fail to improve upon Greedy-ML after the leakage correction. The near-identical performance of BSDS-Recursive and BSDS-NoAug confirms that recursive feature augmentation is negligible. The similar performance of Greedy-MLP-NN (standard BCE loss) and BSDS-Recursive confirms that the BSDS loss function provides no advantage over cross-entropy, addressing the circularity concern: neither optimizing the evaluation metric nor adding architectural capacity improves upon the RF baseline’s ranking.

5.2 Why LLMs Fail Under Zero-Shot SMILES-Only Evaluation

What the comparison tests. Our evaluation tests the *marginal value* of LLMs given access to an existing ML pipeline—the realistic deployment scenario where a pharmaceutical team already has a trained surrogate model and asks whether an LLM can improve candidate selection. Direct mode tests whether an LLM can match a trained classifier from SMILES alone (a capability ceiling); Rerank mode tests whether an LLM adds orthogonal signal beyond the ML model (the practical question). The comparison is deliberately asymmetric: the RF sees 33,000+ training examples while the LLM receives at most $k=3$ few-shot examples, because this reflects real deployment—the ML model *has* been trained on available data, and the question is whether the LLM contributes additional value.

All 14 zero-shot LLM proposers underperform Greedy-ML. The Direct-mode failure indicates that production LLMs cannot extract discriminative signal from SMILES notation alone in a low-prevalence ($p = 0.035$) screening setting. The zero-shot SMILES-to-activity mapping requires structure–activity reasoning that current LLMs do not perform with sufficient fidelity.

Table 12: Deployment simulation on MoleculeNet HIV: hits, hit rate, and return on investment (ROI) for four ranking strategies across experimental budgets B .

Strategy	B	Hits	Hit Rate	Cost (\$K)	ROI
Random	50	2	3.4%	250	-66%
RF (Greedy-ML)	50	48	96.0%	250	860%
BSDS-Recursive	50	31	62.0%	250	520%
Greedy-MLP-NN	50	39	78.0%	250	680%
Random	200	7	3.5%	1000	-65%
RF (Greedy-ML)	200	172	86.0%	1000	760%
BSDS-Recursive	200	109	54.5%	1000	445%
Greedy-MLP-NN	200	128	64.0%	1000	540%
Random	500	18	3.5%	2500	-65%
RF (Greedy-ML)	500	372	74.4%	2500	644%
BSDS-Recursive	500	232	46.4%	2500	364%
Greedy-MLP-NN	500	272	54.4%	2500	444%

Table 13: Random vs. scaffold split comparison on MoleculeNet HIV. DQS values are budget-averaged over 1,000 bootstrap replicates. Greedy-ML remains the best proposer under both split types.

Proposer	Random DQS	Scaffold DQS
Greedy-ML	-0.046	-0.116
Retrieval	-0.091	-0.163
Ensemble	-0.102	-0.182
Informed-Prior	-0.178	-0.260
BSDS-Guided	-0.234	-0.310
BSDS-1Round	-0.258	-0.321
BSDS-NoAug	-0.296	-0.334
BSDS-Recursive	-0.323	-0.378
Greedy-MLP-NN	-0.315	-0.448
Generative	-0.670	-0.704
Random	-0.819	-0.819

Reranking partially recovers performance because the RF’s predicted probabilities provide an informative prior that the LLM only needs to *refine* rather than construct from scratch. However, even the best rerankers degrade rather than improve the RF’s ranking, as evidenced by their worse DQS compared with Greedy-ML (Table 2). The LLM adds noise to the RF’s discriminative ranking rather than orthogonal signal.

Few-shot evaluation. The few-shot experiments (Section 4.5) show that $k=3$ active and $k=3$ inactive examples provide moderate improvement in Direct mode but only marginal gains in Rerank mode. No few-shot proposer surpasses Greedy-ML. This confirms that calibration examples alone are insufficient to close the LLM-ML gap.

Scope of the negative result. The finding that no LLM surpasses Greedy-ML holds under both zero-shot and few-shot ($k=3$) SMILES-only evaluation with no tool access on both HIV (41,127 compounds) and Tox21 NR-AR-LBD (6,758 compounds), confirming the result is not dataset-specific (Section 4.6). Remaining open directions include: chain-of-thought rea-

soning about molecular properties and functional groups, retrieval-augmented generation with ChEMBL/PubChem literature, and tool-augmented evaluation where LLMs can query docking simulators and ADMET (absorption, distribution, metabolism, excretion, toxicity) predictors. Each of these strategies has been shown to substantially improve LLM performance on scientific reasoning tasks in other domains (Wei et al., 2022; Lewis et al., 2020; Schick et al., 2024).

5.3 Mechanistic Ablation Insights

The ablation proposers reveal which reasoning primitives matter most. **Structural retrieval** (Retrieval) provides the most valuable signal among the ablations by identifying compounds similar to known actives—analogue to scaffold hopping in medicinal chemistry (Hu et al., 2017). **Knowledge priors alone** (Informed-Prior) are insufficient to overcome the RF’s learned features, but complement retrieval when corroborated by structural evidence. **Temperature-based exploration** (Generative) uniformly degrades performance, indicating that perturbation of the ML ranking destroys more signal than exploration recovers. **Ensemble aggregation** (Ensemble) provides moderate gains with lowest bootstrap variance, making it a conservative default when the best individual strategy is unknown a priori. The ablation proposers represent an upper bound on what real LLMs can achieve: the mechanistic ablations outperform or match the best real LLMs at every budget level, suggesting that structured information sources (knowledge priors, structural similarity) are more effective than unstructured LLM reasoning for this task.

5.4 The Value of Formally Verified Evaluation

The results demonstrate three specific ways in which BSDS/DQS improve evaluation reliability. First, budget-sensitive ranking avoids misleading conclusions: DQS and EF@1% produce discordant proposer rankings at generous budgets, and the formal monotonicity guarantee ensures correct reflection of additional true hits at any budget. Second, abstention evaluation rewards conservative selection: the Bayes-optimal threshold $\hat{p} < \gamma/(1 + \lambda) = 0.15$ provides a principled criterion that neither EF nor BEDROC can evaluate. Third, the 20 Lean 4 theorems guarantee that BSDS possesses its stated properties regardless of LLM behavior—critical when evaluating opaque models whose behavior is unpredictable. Standard VS metrics (EF, BEDROC, AUROC) produce identical values for 7 of 8 proposers that share the same RF surrogate; only BSDS/DQS distinguish them.

5.5 Seed-0 vs. Bootstrap Distinction

Seed-0 uses the full dataset without resampling, providing point estimates of per-budget BSDS (Tables 2 and 4). Seeds 1–999 sample with replacement, providing bootstrap distributions that quantify uncertainty in DQS and enable hypothesis testing via paired differences. The distinction matters: Retrieval achieves a higher DQS on seed-0 (full data) than on bootstrap resamples, because bootstrap sampling reduces the effective diversity of the knowledge base.

5.6 Limitations

We acknowledge six limitations. **Limited datasets:** the cross-dataset analysis (Section 4.12) demonstrates moderate rank stability across five MoleculeNet benchmarks spanning 0.18%–46.2% prevalence (mean Kendall $\tau = 0.658$), and the cross-domain analysis (Section 4.13) confirms generalization to AV safety triage (mean $\tau = 0.524$ vs. drug datasets). The lower tau for MUV-466 (vs. other drug datasets) reflects its extreme rarity (27 actives in 14,841 compounds). Remaining gaps include regression targets, multi-objective optimization, and materials science. Parameter sensitivity (Section 4.11) confirms that the proposer hierarchy is robust to (λ, γ) choice (Kendall $\tau \geq 0.636$ across 63 parameter pairs, mean $\tau = 0.863$). **Single baseline model:**

we address this partially with ChemBERTa-2 and MolFormer-XL baselines (Section 4.7), but GNNs remain unexplored. Published GNN results on MoleculeNet HIV (scaffold split) report AUROC = 0.771 for D-MPNN (Yang et al., 2019), 0.757 for AttentiveFP, and up to 0.821 for recent architectures—all below our ECFP4+RF baseline. We report results under both random and scaffold CV splits (Section 4) to ensure the proposer hierarchy is not an artifact of random splitting; the qualitative ranking is preserved. **LLM protocol:** we evaluate both zero-shot and few-shot ($k=3$) modes on two datasets (HIV and Tox21, Sections 4.5–4.6); chain-of-thought (CoT), retrieval-augmented generation (RAG), and tool use remain future work. **Clean knowledge base:** our simulated knowledge base contains only true actives, whereas real LLM training data includes noisy and contradictory annotations. **No wet-lab validation:** all evaluations are computational. **BSDS-Recursive circularity:** with the leakage correction, BSDS-Recursive no longer outperforms Greedy-ML, substantially reducing the circularity concern. Nevertheless, the fact that BSDS-Recursive optimizes the evaluation metric warrants continued scrutiny in other domains or prevalence regimes where the surrogate approximation gap may differ.

Ethical considerations. LLM-guided discovery could in principle be directed toward harmful applications. The proposer strategies in this work operate on existing compound libraries and do not generate novel structures, but integration with generative models could extend scope, motivating community safeguards including access controls and dual-use reporting (Urbina et al., 2022). The BSDS framework provides a partial safety net by penalizing false discoveries, but practitioners must supplement evaluation with domain-specific safety assessments.

5.7 Future Work

Three directions are most pressing. **Advanced LLM prompting:** the few-shot results (Section 4.5) address the most immediate gap; remaining strategies include chain-of-thought molecular reasoning, RAG with ChEMBL/PubChem, and tool-augmented evaluation (docking, ADMET prediction). The open question is whether structured molecular reasoning—rather than broader parametric knowledge—can close the gap with Greedy-ML. **Broader cross-domain evaluation:** the cross-dataset analysis (Section 4.12) demonstrates generalization across five classification tasks spanning 0.18%–46.2% prevalence (mean Kendall $\tau = 0.658$), and the AV Safety analysis (Section 4.13) confirms cross-domain transfer (mean $\tau = 0.524$); extending to regression targets, materials science, climate risk, and financial applications requires only changing the data loader and hit function. **Multi-objective extension:** real discovery optimizes potency, selectivity, ADMET, and synthetic accessibility simultaneously; extending BSDS to conjunctive thresholds on multiple properties is straightforward in principle but requires multi-endpoint datasets.

6 Conclusion

We introduced the Budget-Sensitive Discovery Score (BSDS), a formally verified evaluation framework (20 Lean 4-checked theorems) for comparing candidate selection strategies under realistic budget constraints and asymmetric error costs. As a case study, we evaluated 39 proposer strategies—11 mechanistic variants (including 3 ablation controls), 14 zero-shot LLM configurations (7 models \times 2 modes), and 14 few-shot LLM configurations—on MoleculeNet HIV (41,127 compounds, 3.5% active, 1,000 bootstrap replicates) under both random and scaffold CV splits, with cross-dataset validation on four additional MoleculeNet benchmarks spanning 0.18%–46.2% prevalence and cross-domain validation on AV safety triage (30,000 scenarios).

Five findings emerge. First, the simple RF-based Greedy-ML proposer ($DQS = -0.046$) outperforms all 10 other mechanistic proposers and all 28 LLM configurations; additional MLP

reranking layers degrade rather than improve the RF’s discriminative ranking, and a deployment simulation confirms that Greedy-ML achieves a 96% hit rate at $B = 50$ versus 78% for the best MLP variant. Second, ablation analysis shows that neither the BSDS loss function, MLP capacity, nor recursive feature augmentation can improve upon the RF baseline, with all four MLP variants performing worse than Greedy-ML. Third, no production LLM surpasses the Greedy-ML baseline under zero-shot or few-shot SMILES evaluation on either HIV or Tox21; all direct-mode LLMs perform near-random. Fourth, BSDS/DQS reveal budget-dependent trade-offs invisible to standard virtual screening metrics: multiple proposers with identical EF and AUROC values produce substantially different DQS. Fifth, the proposer hierarchy generalizes across datasets and domains: the ranking is broadly stable across five MoleculeNet benchmarks, with consistent qualitative ordering on the non-drug AV Safety domain; and $\tau \geq 0.636$ across a 9×7 grid of (λ, γ) parameters (mean $\tau = 0.863$).

The broader contribution is the evaluation framework itself. The BSDS framework applies in principle to any setting where candidates are selected under budget constraints and asymmetric error costs—drug discovery, materials screening, safety triage, clinical trial planning—as demonstrated here across pharmaceutical screening and autonomous vehicle safety triage. Whether LLMs help, hurt, or make no difference, the framework provides the rigorous, budget-sensitive evaluation needed to know for certain. Remaining open directions include chain-of-thought reasoning, RAG, tool-augmented evaluation, and domain-specific LLM fine-tuning.

References

- Walid Ahmad, Elana Simon, Seyone Chithrananda, Gabriel Grand, and Bharath Ramsundar. ChemBERTa-2: Towards chemical foundation models. *arXiv preprint arXiv:2209.01712*, 2022.
- Abhinaba Basu and Pavan Chakraborty. The budgeted selective discovery score: A formally verified, domain-agnostic metric for evaluating scientific discovery under budget constraints. *Manuscript in preparation*, 2025. 20 theorems machine-checked in Lean 4.
- Guy W. Bemis and Mark A. Murcko. The properties of known drugs. 1. molecular frameworks. *Journal of Medicinal Chemistry*, 39(15):2887–2893, 1996. doi: 10.1021/jm9602928.
- Daniil A. Boiko, Robert MacKnight, Ben Kline, and Gabe Gomes. Autonomous chemical research with large language models. *Nature*, 624(7992):570–578, 2023. doi: 10.1038/s41586-023-06792-0.
- Andres M. Bran, Sam Cox, Oliver Schilter, Carlo Baldassari, Andrew D. White, and Philippe Schwaller. Augmenting large language models with chemistry tools. *Nature Machine Intelligence*, 6(5):525–535, 2024. doi: 10.1038/s42256-024-00832-8.
- Davide Chicco and Giuseppe Jurman. The advantages of the Matthews correlation coefficient (MCC) over F1 score and accuracy in binary classification evaluation. *BMC Genomics*, 21(1):6, 2020. doi: 10.1186/s12864-019-6413-7.
- Leonardo de Moura and Sebastian Ullrich. The Lean 4 theorem prover and programming language. In *Proceedings of the 28th International Conference on Automated Deduction (CADE-28)*, pages 625–635, 2021. doi: 10.1007/978-3-030-79876-5_37.
- Bradley Efron. Better bootstrap confidence intervals. *Journal of the American Statistical Association*, 82(397):171–185, 1987. doi: 10.1080/01621459.1987.10478410.
- David E. Graff, Eugene I. Shakhnovich, and Connor W. Coley. Accelerating high-throughput virtual screening through molecular pool-based active learning. *Chemical Science*, 12(22):7866–7881, 2021. doi: 10.1039/D0SC06805E.

- Ye Hu, Dagmar Stumpfe, and Jürgen Bajorath. Recent advances in scaffold hopping. *Journal of Medicinal Chemistry*, 60(4):1238–1246, 2017. doi: 10.1021/acs.jmedchem.6b01437.
- Ruili Huang, Menghang Xia, Dac-Trung Nguyen, Tongan Zhao, Srilatha Sakamuru, Jinghua Zhao, Sampada A. Shahane, Anna Rossoshek, and Anton Simeonov. Tox21 challenge to build predictive models of nuclear receptor and stress response pathways as mediated by exposure to environmental chemicals and drugs. *Frontiers in Environmental Science*, 3:85, 2016. doi: 10.3389/fenvs.2015.00085.
- Kevin Maik Jablonka, Philippe Schwaller, Andres Ortega-Guerrero, and Berend Smit. Is GPT-4 a good data analyst? a benchmark for large language models in chemistry. *arXiv preprint arXiv:2402.13654*, 2024.
- Ajay N. Jain and Anthony Nicholls. Recommendations for evaluation of computational methods. *Journal of Computer-Aided Molecular Design*, 22(3–4):133–139, 2008. doi: 10.1007/s10822-008-9196-5.
- Michael Kuhn, Ivica Letunic, Lars Juhl Jensen, and Peer Bork. The SIDER database of drugs and side effects. *Nucleic Acids Research*, 44(D1):D1075–D1079, 2016. doi: 10.1093/nar/gkv1075.
- Patrick Lewis, Ethan Perez, Aleksandara Piktus, Fabio Petroni, Vladimir Karpukhin, Naman Goyal, Heinrich Küttler, Mike Lewis, Wen-tau Yih, Tim Rocktäschel, Sebastian Riedel, and Douwe Kiela. Retrieval-augmented generation for knowledge-intensive NLP tasks. In *Advances in Neural Information Processing Systems (NeurIPS)*, volume 33, pages 9459–9474, 2020.
- Haoqiang Ma, Chengkun Yan, Yutong Guo, Changsheng Wang, Haiping Zhang, Xuanyu Wang, and Zhaoping Zhang. The rise of AI in drug design: Review of LLM-based drug design. *arXiv preprint arXiv:2406.08426*, 2024.
- Ricardo Macarron, Martyn N. Banks, Dejan Bojanic, David J. Burns, Dragan A. Cirovic, Tina Garyantes, Darren V. S. Green, Robert P. Hertzberg, William P. Janzen, Jeff W. Paslay, Ulrich Schopfer, and G. Sitta Sittampalam. Impact of high-throughput screening in biomedical research. *Nature Reviews Drug Discovery*, 10(3):188–195, 2011. doi: 10.1038/nrd3368.
- Bharath Ramsundar, Peter Eastman, Patrick Walters, and Vijay Pande. *Deep Learning for the Life Sciences*. O’Reilly Media, 2019. ISBN 978-1-492-03983-9.
- Daniel Reker and Gisbert Schneider. Active-learning strategies in computer-assisted drug discovery. *Drug Discovery Today*, 20(4):458–465, 2015. doi: 10.1016/j.drudis.2014.12.004.
- David Rogers and Mathew Hahn. Extended-connectivity fingerprints. *Journal of Chemical Information and Modeling*, 50(5):742–754, 2010. doi: 10.1021/ci100050t.
- Sebastian G. Rohrer and Knut Baumann. Maximum unbiased validation (MUV) data sets for virtual screening based on PubChem bioactivity data. *Journal of Chemical Information and Modeling*, 49(2):169–184, 2009. doi: 10.1021/ci8002649.
- Bernardino Romera-Paredes, Mohammadamin Barekatian, Alexander Novikov, Matej Balog, M. Pawan Kumar, Emilien Dupont, Francisco J. R. Ruiz, Jordan S. Ellenberg, Pengming Wang, Omar Fawzi, Pushmeet Kohli, and Alhussein Fawzi. Mathematical discoveries from program search with large language models. *Nature*, 625(7995):468–475, 2024. doi: 10.1038/s41586-023-06924-6.
- Jerret Ross, Brian Belgodere, Vijil Chenthamarakshan, Inkit Padhi, Youssef Mroueh, and Payel Das. Large-scale chemical language representations capture molecular structure and properties. *Nature Machine Intelligence*, 4(12):1256–1264, 2022. doi: 10.1038/s42256-022-00580-7.

- Timo Schick, Jane Dwivedi-Yu, Roberto Dessì, Roberta Raileanu, Maria Lomeli, Eric Hambro, Luke Zettlemoyer, Nicola Cancedda, and Thomas Scialom. Toolformer: Language models can teach themselves to use tools. *Advances in Neural Information Processing Systems (NeurIPS)*, 36, 2024.
- Daniel Selsam, Percy Liang, and David L. Dill. Developing bug-free machine learning systems with formal mathematics. *Proceedings of the 34th International Conference on Machine Learning (ICML)*, 70:3047–3056, 2017.
- Burr Settles. Active learning literature survey. *Computer Sciences Technical Report 1648, University of Wisconsin–Madison*, 2009.
- Jean-François Truchon and Christopher I. Bayly. Evaluating virtual screening methods: Good and bad metrics for the “early recognition” problem. *Journal of Chemical Information and Modeling*, 47(2):488–508, 2007. doi: 10.1021/ci600426e.
- Fabio Urbina, Filippa Lentzos, Cedric Invernizzi, and Sean Ekins. Dual use of artificial-intelligence-powered drug discovery. *Nature Machine Intelligence*, 4(3):189–191, 2022. doi: 10.1038/s42256-022-00465-9.
- Jessica Vamathevan, Dominic Clark, Paul Czodrowski, Ian Dunham, Edgardo Ferran, George Lee, Bin Li, Anant Madabhushi, Parantu Shah, Michaela Spitzer, and Shanrong Zhao. Applications of machine learning in drug discovery and development. *Nature Reviews Drug Discovery*, 18(6):463–477, 2019. doi: 10.1038/s41573-019-0024-5.
- Jason Wei, Xuezhi Wang, Dale Schuurmans, Maarten Bosma, Brian Ichter, Fei Xia, Ed H. Chi, Quoc V. Le, and Denny Zhou. Chain-of-thought prompting elicits reasoning in large language models. In *Advances in Neural Information Processing Systems (NeurIPS)*, volume 35, pages 24824–24837, 2022.
- Zhenqin Wu, Bharath Ramsundar, Evan N. Feinberg, Joseph Gomes, Caleb Geniesse, Aneesh S. Pappu, Karl Leswing, and Vijay Pande. MoleculeNet: A benchmark for molecular machine learning. *Chemical Science*, 9(2):513–530, 2018. doi: 10.1039/C7SC02664A.
- Kevin Yang, Kyle Swanson, Wengong Jin, Connor Coley, Philipp Eiden, Hua Gao, Angel Guzman-Perez, Timothy Hopper, Brian Kelley, Miriam Mathea, Andrew Palmer, Volker Settels, Tommi Jaakkola, Klavs Jensen, and Regina Barzilay. Analyzing learned molecular representations for property prediction. *Journal of Chemical Information and Modeling*, 59(8): 3370–3388, 2019. doi: 10.1021/acs.jcim.9b00237.